Chemistry—Methods

Research Article
doi.org/10.1002/cmtd.202400093

Chemistry Europe
European Chemical Societies Publishing

www.chemistrymethods.org

Analytical Study of Lanolin as Potential Biomarker of Prehistoric Sheep-Shearing Practice

Claudia Adsuar Fuster, Francesco Caruso,* Olivia Gómez-Laserna, Martina Romani, Ramón J. Barrio, Josep Maria Vergès, Vincenza Forgia, Maite Maguregui,* and Asier Vallejo*

Sheep-shearing practices probably started in the Neolithic Age when the genetic selection of sheep began to be successful in obtaining animals with abundant wool. Flint and obsidian were the main materials probably used to manufacture tools for this purpose. From shearing, lanolin wax is accumulated onto the shearing tools. Lanolin is a complex mixture of esters and polyesters, alcohols, fatty acids, and hydrocarbons produced mainly by sheep to protect the skin and the wool from environmental agents. Due to its complex chemistry, lanolin is relatively difficult to characterize. This work investigates the possible use of lanolin as a biomarker of sheep-shearing practices in the prehistoric era. For this purpose, lanolin degradation pathways have been studied by an experimental archeology approach adjuvated by Fourier transformed infrared spectroscopy, hyperspectral imaging, and gas chromatography coupled with mass spectrometry.

1. Introduction

Nowadays, sheep shearing is a practice required at least once a year (usually carried out in the summer) to remove wool from sheep, keeping them cool and reducing the presence of parasites.[1,2] Sheep-shearing practices probably started in the Near East at an advanced stage of the Neolithic period (4th to 3rd millennium BCE), when the genetic selection of sheep, aimed at obtaining breeds with abundant wool, began to bear fruit.[3] Sheep and goats—together with cattle and pigs—were the main species of domesticated animals in this period.[4,5] Sheep conveniently adapted to multiple environments and provided a wide array of commodities and services, including meat, hide, and bone. Thereafter, secondary products, such as milk and fiber were intensely exploited.[2,6,7] The earliest breed of sheep still had very short, strong hair. Afterwards, new breeds of woolly sheep emerged and were introduced in Central Europe possibly from the Eastern Mediterranean, leading to the start of wool production. The first archeological evidence of a fully developed wool economy in continental Europe dates from the 2nd millennium BCE.[2,8,9] It was then possible to obtain wool (secondary product) from the same sheep multiple times, without the need to kill it to obtain its hide.[6,10]

For all these activities (namely, hunting, domestication, agriculture, and manufacturing), stone tools were used from the Neolithic to the Bronze Age. Among them, lithic artifacts, made of flint and obsidian (mostly used in volcanic areas), were common materials used for cutting, being the most likely shearing tools.[11]

During sheep shearing, a natural wax called lanolin accumulates on the tools. This wax protects wool from environmental agents (such as sunlight, wind, or rain), and represents 10–25% of the mass of freshly sheared wool.[12,13] Lanolin is a complex mixture of high molecular weight esters and polyesters (87% of a typical lanolin sample), alcohols (aliphatic alcohols, sterols, and trimethyl sterols), fatty acids, and hydrocarbons.[14,15] Cholesterol, lanosterol, and dihydrolanosterol (lanostenol) are three important components of lanolin,[16,17] among others.

Nowadays, lanolin is widely employed in the cosmetic industry and is a common ingredient in topical medications.[18,19] It also has many applications in industry as a coater and polisher for metallic surfaces,[20] furniture,[21] clothing, and footwear.[15]

Despite its several uses, lanolin is challenging to characterize due to its fraction of unidentified compounds and its variable composition. Breeds of sheep, geographical origin, degradation

C. Adsuar Fuster, F. Caruso, R. J. Barrio, M. Maguregui, A. Vallejo
Department of Analytical Chemistry, Faculty of Pharmacy
University of the Basque Country UPV/EHU Paseo de la Universidad 7
01006 Vitoria-Gasteiz, Spain
E-mail: francesco.caruso@ehu.eus
maite.maguregui@ehu.eus
asier.vallejo@ehu.eus

O. Gómez-Laserna, M. Romani
Department of Analytical Chemistry, Faculty of Science and Technology
University of the Basque Country UPV/EHU
Barrio Sarriena s/n, 48840 Leioa, Spain

J. M. Vergès
Catalan Institute of Human Paleoecology and Social Evolution (IPHES-CERCA)
Zona Educacional 4
Campus Sescelades (Edifici W3), 43007 Tarragona, Spain

J. M. Vergès
Department of History and Art History
Universitat Rovira i Virgili
Avinguda de Catalunya 35, 43002 Tarragona, Spain

V. Forgia
Department of Cultures and Society
University of Palermo
Viale delle Scienze Edificio 15, 90128 Palermo, Italy

Supporting information for this article is available on the WWW under https://doi.org/10.1002/cmtd.202400093

Research Article
doi.org/10.1002/cmtd.202400093
Chemistry Europe
European Chemical Societies Publishing

time, extraction, and purification methods may all contribute to different chemical profiles of lanolin.[14] Nevertheless, as the origin of lanolin is peculiar and some of its compounds can survive weathering and aging, this wax could be a good biomarker for prehistoric sheep-shearing practices.

Archeological biomarkers are persistent organic compounds, such as lipids, proteins, and polynucleotides, present in the archeological record. They can be related to a certain origin and are therefore useful to describe aspects of the human development throughout history.[22,23] These compounds must be relatively resistant to degradation and chemically stable over long periods. It is however not trivial to find new biomarkers.[23] First, there is the issue of **persistence**, as many of these biomolecules are susceptible to chemical and physical alteration over time.[24] Second, **specificity** plays an important role in current archeological science research, since certain compounds may not come from a particular source but may have multiple origins,[25,26] as it is common in the case of lipids.

Degradation phenomena may be triggered by different factors: chemical, physical (electromagnetic radiation, temperature, relative humidity), and biological agents.[27,28] For this reason, their study is valuable to assess whether some compounds (or their characteristic transformation products) are likely to survive over ample timescales. These studies can be approached by laboratory experimentation, subjecting the compounds of interest to artificial aging to characterize the resulting degradation products.

Under the experimental archeology perspective, the development of a procedure to study a degradation phenomenon has to be carried out preferably under conditions as close as possible to the real ones and within a reasonable timeframe.[29,30] With these considerations in mind, an approach for monitoring the aging of lanolin in samples from archeological sites has been developed in the present work. Since lanolin is expected to remain in the cutting tools used for shearing, lanolin degradation pattern was studied on lithic tools with the approach mentioned earlier. For this purpose, different types of contemporary flint and obsidian fragments were selected as potential shearing tools. Red flint fragments from Montsant (Tarragona, Catalonia, Spain), black flint fragments from Monegros (Huesca, Aragon, Spain), and obsidian fragments from the island of Lipari (Messina, Sicily, Italy) were employed. The choice of flint and obsidian as experimental blades covers most of the materials used from the Neolithic to the Bronze Age in the manufacture of cutting tools.

One of the main techniques used for the noninvasive chemical study of organic residues is micro-Fourier transform infrared spectroscopy (FTIR) in reflectance.[31–33] In a similar way, hyperspectral imaging (HSI) has emerged as a powerful spectroscopic technique in the last decades, effectively combining spectral and spatial information. HSI complements the micro-FTIR analysis in terms of spectral range, since it operates in the short wave infrared (SWIR) region (1000–2500 nm).[34]

For organic residue analysis that involves complex mixtures, chromatographic and mass spectrometric methods are imperative.[25] Gas chromatography coupled with mass spectrometry (GC-MS) is the preferred technique for separation and characterization of the mixture due to its robustness and its very low detection limits. In non-targeted analysis, GC-MS enables the identification of the unknown compounds in the sample by comparison with spectral libraries. In this work, the degradation pathway of lanolin has been studied by the controlled application of this wax on the previously mentioned clean flint and obsidian fragments. Lanolin has been progressively aged in a climatic chamber, and the degradation pattern has been investigated by non-destructive and micro-destructive analytical methods. For that, micro-FTIR in reflectance, HSI in the SWIR range and GC-MS were employed.

2. Results and Discussion

2.1. Micro-FTIR of Clean Flint and Obsidian Fragments

Spectra obtained from five pieces of each type of flint and obsidian exhibited similar trends, hence the average was considered for the spectra analysis.

Both flint and obsidian showed an intense band around 1120 cm^{-1} typically attributed to Si-*O*-Si stretching,[35,36] much more intense in flint pieces compared to obsidian pieces (**Figure 1**).

Difference in the intensity of this band may be attributed to the material's structure, as obsidian is an amorphous solid, a glass, and flint presents a cryptocrystalline structure, formed of a mixture of amorphous and crystalline silica. It might also be due to the silica content (typical silica content of a flint: $\geq$90%; typical silica content of an obsidian $\approx$70%).[37–39] Differences in spectra may also be due to variations in surface irregularity or material translucency.

A "reststrahlen" signal was observed in the 1200–1400 cm^{-1} region. Weak interference from atmospheric CO_2 and H_2O was observed around 2350 cm^{-1} and 3500–4000 cm^{-1}, respectively. Due to the black glassy surface, the spectra of the obsidian fragments showed higher noise with respect to the ones of the flint fragments.

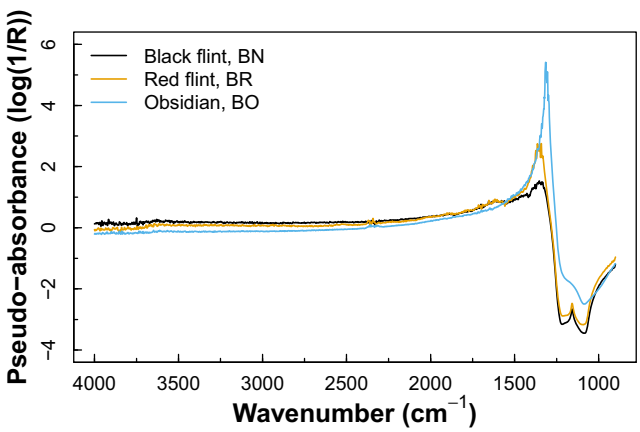

Figure 1. Reflectance FTIR spectra of clean flint (BN and BR) and obsidian (BO) fragments. Applied pre-processing: SNV correction, average of 12 measurements for BR (on 4 fragments) and of 15 measurements for BN and BO (on 5 fragments each).

Research Article
doi.org/10.1002/cmtd.202400093
Chemistry Europe
European Chemical Societies Publishing

2.2. Micro-FTIR of Unaged and Aged Lanolin-Treated Flint and Obsidian Fragments

After the application of the solution of lanolin on the fragments, the mass per surface area was calculated, as shown in **Table 1**.

Mass per surface area values ranged between around 0.4 and 0.9 mg cm^{-2}, except for the value of MR_01 being by far the highest. MR_01 was the first fragment to be brushed with the solution of lanolin. Its application was probably not as controlled as with the other fragments, so an excess of lanolin was applied. After applying the ISO-recommended Grubbs' test with $P = 0.05$ for this outlier,[40] a mean value of mass per surface area of (0.60 ± 0.17) mg cm^{-2} ($n = 14$) was obtained. The median value was 0.57 mg cm^{-2}. The mean and median of the measurements taken on the 14 samples are therefore very close (relative difference of 5%), indicating that the data of Table 1, without the contribution given by the value of MR_01, is mostly symmetrically distributed with minimal skewness.

The FTIR spectra of lanolin-treated samples showed a different aspect from the spectra of the clean fragments (**Figure 2**).

Intense bands at 2847 and 2915 cm^{-1} were observed due to the —CH_3 and —CH_2 stretching vibrations of methyl and methylene hydrogen, as well as the methylene scissoring mode of lipids at 1474 cm^{-1} and another bending vibration of methyl and methylene hydrogen at 1382 cm^{-1}. Other authors assign the band at 1374 cm^{-1} (in spectra acquired in attenuated total reflectance) to the O—CH_2 vibration in mono-, di-, or triglycerides.[41,42] A peak at 1738 cm^{-1} was also observed due to the presence of the carbonyl group of the fatty acid esters from lanolin.[42–44] It is as well noteworthy the increased intensity of silica band in obsidian from clean fragments to lanolin-treated samples. This may be associated with the contribution of lanolin to the obsidian FTIR spectrum around the 1100 cm^{-1} region.[43,45] In this region it could be observed the stretching vibration bands of the ester linkage in triglycerides,[46] symmetrical C—O—C stretching, asymmetrical —C—H bending and —OH stretching.[44] The CO— stretching due to primary, secondary, or tertiary alcohols seems however to be the most valid hypothesis of lanolin contribution to the increase of silica band in lanolin-treated obsidian samples.[47,48]

Table 1. Values of mass of applied lanolin, estimation of the surface area of one of the sides of the samples and mass per surface area. MR_##, lanolin-treated red flint fragments; MN_##, lanolin-treated black flint fragments; MO_##, lanolin-treated obsidian fragments.

Sample	Applied lanolin [mg]	Surface area [cm^2]	Mass of lanolin per surface area [mg cm^{-2}]
MR_01	23.83	17.487	1.36
MR_02	5.14	10.790	0.48
MR_03	6.20	13.435	0.46
MR_04	6.47	9.678	0.67
MR_05	4.40	7.814	0.56
MN_01	5.54	10.191	0.54
MN_02	6.31	14.740	0.43
MN_03	6.85	11.763	0.58
MN_04	6.26	8.971	0.70
MN_05	2.21	6.250	0.35
MO_02	5.71	7.089	0.81
MO_03	5.57	6.941	0.80
MO_04	2.65	5.279	0.50
MO_05	5.01	5.330	0.94
MO_06	2.45	3.845	0.64

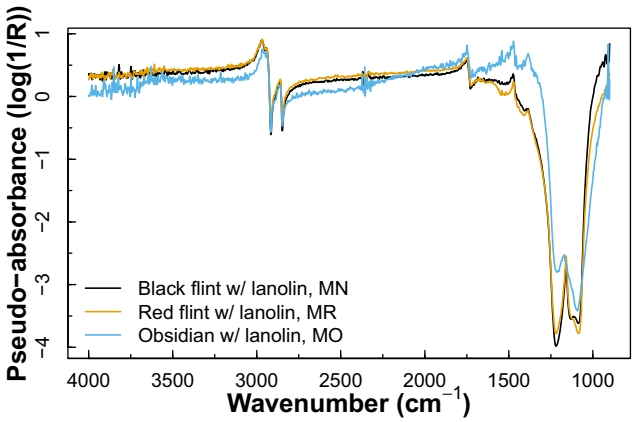

Figure 2. Reflectance FTIR spectra of flint (MN and MR) and obsidian (MO) fragments treated with lanolin. Applied pre-processing: SNV correction, average of 15 measurements for MN and MR (on 5 fragments), and of 21 measurements for MO (on 5 fragments).

The spectra of the fragments with artificially aged lanolin showed some differences with respect to the ones of the fragments with unaged lanolin. A slight increase in the intensity of the carbonyl band at 1738 cm^{-1} was recorded in both flint and obsidian samples with the progression of aging (**Figure 3**).

The increase of this band could suggest the formation of aliphatic aldehydes due to the decomposition of alcohols.[49] The spectra of the aged black flint (Figure 3a) showed a band at 1547 cm^{-1}, appearing after 21 days of aging. The very same band was also observed after 28 days of aging of lanolin on the red flint samples (Figure 3b). Different interpretations of this band are discussed in literature: C=C bond of aromatic ring in 1500–1600 cm^{-1} region,[43] —CH bending mode,[44] typical organic acids/carboxylates bands at 1538–1585 cm^{-1} region.[31,50] Since this band is only found in the spectra of the fragments with the longer aging times, the formation of acids from the breaking down of esters is a valid hypothesis for its origin.

Furthermore, some peculiarities in the spectra of the aged obsidian fragments treated with lanolin were noticed (Figure 3c). Bands with different intensity over aging in methyl and methylene hydrogen vibration 2800–3000 cm^{-1} region were observed. Also here, the contribution of lanolin to the spectrum of the obsidian samples could be confirmed in aged samples due to the change in the shape of the silica band (around 1120 cm^{-1}) with increasing aging times.

As in the case of the spectra of the clean fragments, due to the surface characteristics, the spectra of the lanolin-treated obsidian fragments showed higher noise with respect to the ones of the lanolin-treated flint fragments.

In some of the measured spots, the characteristic spectral pattern of clean flint or obsidian was observed. This may be due to

Research Article
doi.org/10.1002/cmtd.202400093
Chemistry Europe
European Chemical Societies Publishing

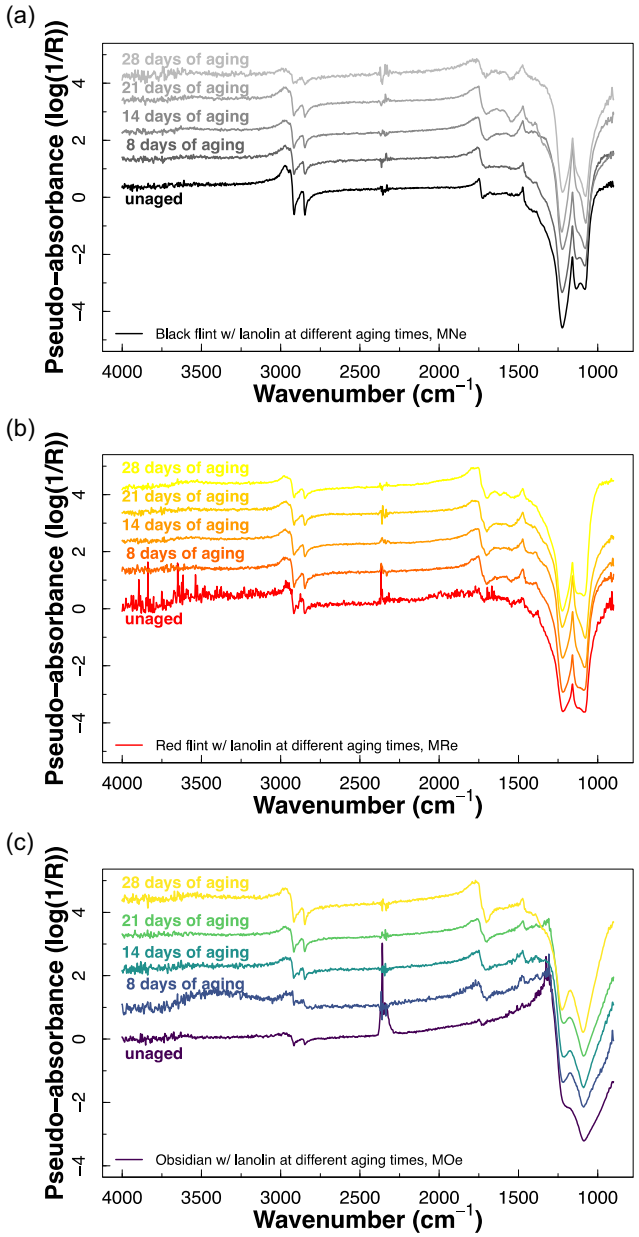

Figure 3. Reflectance FTIR spectra of aged flint (MNe and MRe, a,b) and obsidian (MOe, c) fragments treated with lanolin. Applied pre-processing: SNV correction, average of 3–5 measurements for each aging time.

the manual brushing and irregularity of the fragments, so that a homogeneous distribution of lanolin is not achieved on the whole surface of these fragments. These spectra were not included in the analysis.

2.3. HSI of Unaged and Aged Lanolin-Treated Flint and Obsidian Fragments

The HSI analysis only provided relevant information on black flint samples, due to the inherent characteristics (mainly, color and gloss) of the other samples.

It was proved that the color and surface appearance of the fragments had an influence on the detection of lanolin by HSI in the NIR-SWIR. Lanolin was not detected in obsidian samples, probably because they are too dark and bright. Lanolin was detected in the lighter areas of the MN_03 and MN_04 fragments and much less easily in the rest of the surface with a darker appearance. Lanoline was neither detected in red flints.

As represented in **Figure 4**a, lanolin accumulated at the edges (red color) of unaged black flint samples, as they were usually thicker in the center and thinner on the edges. The highest detection of lanolin was achieved in the white areas of MN_03 and MN_04 pieces. These areas were the only ones in which lanolin was detected by HSI after their aging.

The identification of lanolin was obtained by a spectral correlation model from the pure lanolin standard with the darker and the whiter areas of MN_03 and MN_04 (Figure 4b). A spectral comparison of clean surface, unaged lanolin-treated surface, and aged lanolin-treated surface was made.

In the endmember reflectance spectra of the clean surfaces (BN white and dark areas, **Figure 5**), two main characteristic reflectance minima at 1422 and 1923 nm appear, corresponding to unbound water and crystalline water, respectively, typical of silica. These bands were also observed in the spectra of the unaged and aged lanolin-treated samples. Also, a less pronounced peak at 2200 nm could be attributed to the Si-OH (silanol group) band. The shape of the clean flint spectra and the position of these bands could be associated with the presence of quartz in the material.[51,52]

The spectrum of pure lanolin showed a strong, characteristic feature with minima at 1728 nm and 1762 nm, associated to C—H bonds of triglycerides.[53] This feature was identified with much less intensity in the spectra of the white and dark areas of the unaged sample. Two more contiguous bands at 2311 and 2350 nm, typical of lipids, were observed in the spectra of the unaged sample, although they are not present in the spectrum of the lanolin reference.[54] These mentioned lipid bands were slightly noticed in the spectrum of the white area in the aged

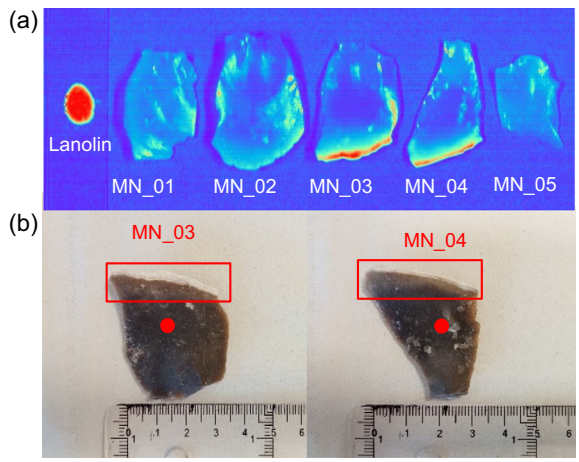

Figure 4. a) Representation of the spectral correlation model of lanolin with the treated fragments. MN_05 is the treated sample with unaged lanolin, MN_03, MN_04, MN_01, and MN_02 are aged for 8, 14, 21, and 28 days, respectively. b) Visible images of fragments MN_03 and MN_04 where the zone at highest and lowest spectral correlation are indicated by a red rectangle and a full red dot, respectively.

Research Article
doi.org/10.1002/cmtd.202400093
Chemistry Europe
European Chemical Societies Publishing

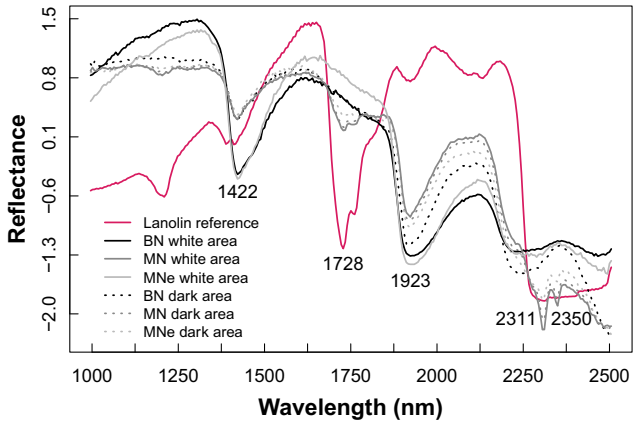

Figure 5. Endmember reflectance spectra of lanolin reference (magenta solid line) and the white (solid lines) and dark (dotted lines) areas of unaged and aged lanolin-treated black flint fragments. Applied pre-processing: SNV. Some characteristic spectral features are also highlighted.

sample. No lanolin features were present in the spectrum of the dark area in the aged sample. Also, a band at 1209 nm, attributed to hydrocarbons, was present in the spectrum of pure lanolin, but was not detected in the spectra of the lanolin-treated samples.[55,56]

Consequently, results show that the detection of lanolin by HSI is relatively limited. Lanolin has a melting point around 36–42 °C.[14] At the temperature applied during the aging (40 °C), partial melting of lanolin could have occurred, causing its partial removal from the surface of the fragments. This should be confirmed by future systematic tests, where aging experiments could be carried out at lower temperature values.

2.4. GC-MS of Lanolin-Treated Flints

A GC-MS study was carried out to determine possible degradation compounds of lanolin, when applied to flint fragments. Both red and black lanolin-treated flint fragments that underwent artificial aging were analyzed. Lanosterol and cholesterol, as main sterols of natural lanolin, were expected to be detected.[17] Unaged samples showed more than 70 different peaks in the total ion chromatograms (TICs) (**Figure 6**), among which carboxylic acids, dicarboxylic acids, and alcohols were found. However, many of these compounds could not be identified because the identification accuracies were below 70% or they were not present in the NIST database

The compounds present in the blank were discarded for study and those with possible different accumulation sources were not selected. Common saturated fatty acids such as palmitic acid or stearic acid were discarded as well, due to their multiple both animal and vegetable origins compatible with their presence in this type of archeological samples (lack of specificity).[57]

The presence of the compound in the sample was confirmed by giving a signal equal to the blank signal plus three standard deviations of the blank.

A first injection in scan mode revealed a region of interest in the superimposed chromatograms of the unaged and aged samples, depicted in **Figure 7** (t_R: 33.7–35.2 min).

As expected, lanosterol and cholesterol, as well as their derivates, such as lanost-8-en-3-ol (3β), (3β)-lanosta-7,9(11),24-trien-3-ol and desmosterol were the main compounds identified in unaged sample (see Figure 6 and **Table 2**).

The signal of these compounds decreased over time as they aged, eventually disappearing (see **Figure 7**–**9**).

Other compounds, possibly with a sterol structure (see Figure 1 in Supporting Information), were observed at similar retention times and mass spectra during longer aging periods. The unequivocal identification of these compounds was not possible due the lack of correspondence with the NIST database. Therefore, a deeper study of the mass spectra must be done to determine the degradation compounds and their source. Besides, their abundance does not follow a trend according to the aging time (Figure 8).

Nevertheless, these compounds are detected in all the aged samples, and these unidentified compounds could—in principle—be proposed as biomarkers for ancient shearing. The missed

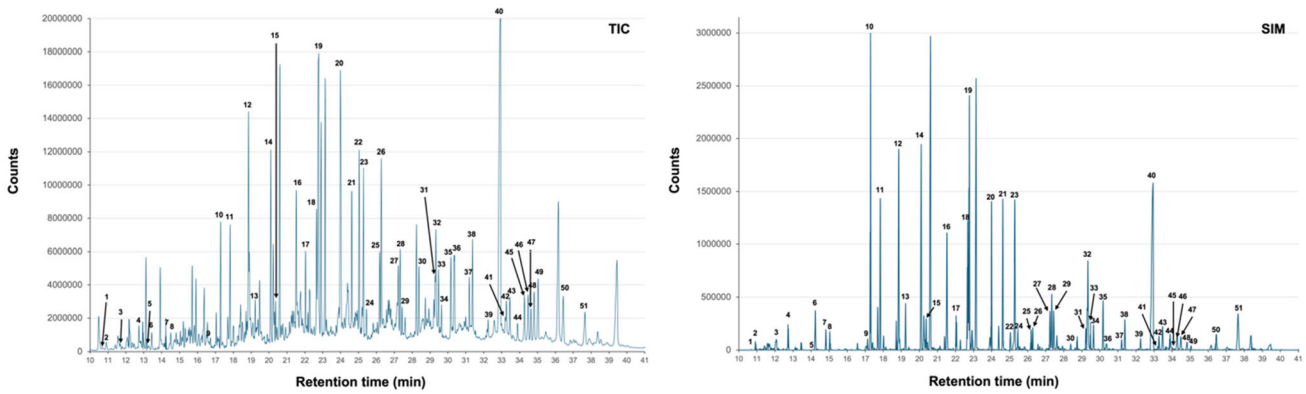

Figure 6. Total ion (TIC, left) and selected ion monitored (SIM, right) chromatograms of MN_05 unaged black flint sample. Peaks identification using NIST library in TICs and corroboration in SIM by retention time and characteristic ions. The compounds not identified with certainty are marked with a*. List of numbered compounds not represented in Table 2, identified in the chromatogram by retention time, collected and classified by functional group: **Dicarboxylic acids:** 1 – Pentanedioic acid, 3 – Hexanedioic acid, 5 – Pimelic acid, 9 – Azelaic acid. **Carboxylic acids**: 2 – 8-Methylnonanoic acid, 4 – Undecanoic acid, 7 – Dodecanoic acid, 11 – Myristic acid, 12 – Pentadecanoic acid*, 13 – Pentadecanoic acid*, 16 – Heptadecanoic acid, 22 – Arachidic acid*, 24 – Arachidic acid*, 26 – Heneicosanoic acid, 27 – Behenic acid, 30 – Tricosanoate, 31 – Lignoceric acid*, 34 – Lignoceric acid*, 36 – Pentacosanoic acid. **Alcohols**: 8 – 1-Tridecanol, 15 – 1-Heptadecanol, 29 – 1-Tricosanol, 33 – 22-Methyltetracosanol, 38 – 1-Heptacosanol. Diols: 17 – Hexadecane-1,2-diol, 20 – Octadecane-1,2-diol, 25 – 18-Methyl-nonadecane-1, 2-diol. **Unidentified peaks**: 6, 10, 14, 18, 18, 21, 28, 32, 35, 37, 39.

Research Article
doi.org/10.1002/cmtd.202400093
Chemistry Europe
European Chemical Societies Publishing

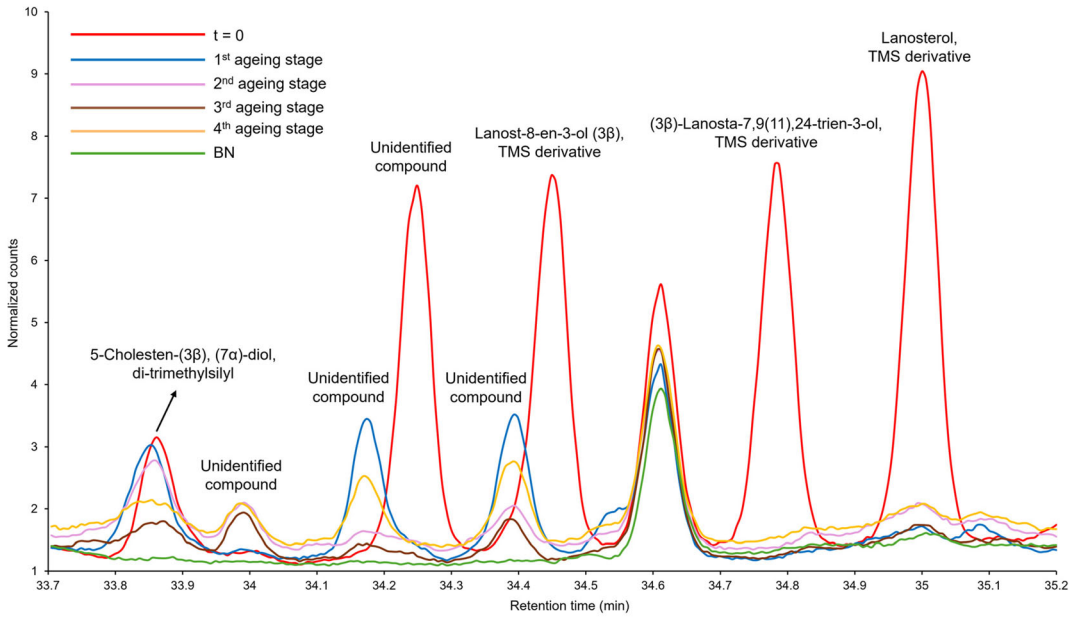

Figure 7. Region of the TIC of characteristic compounds of natural lanolin and related compounds of interest identified in extracted unaged ($t = 0$) and aged black flint samples.

Table 2. Characteristic compounds of natural lanolin and related compounds of interest identified in samples. Retention times (t_R) and characteristic ions. Compounds that were not identified with certainty are marked with *. The peak number refers to the TIC and SIM chromatograms (Figure 6).

Peak number	Compound	t_R [min]	Main fragments [m/z]
23	1-Heneicosanol (TMS)	25.254	369, 383, 75
40	Cholesterol (TMS)	32.854	329, 368, 458
41	(3β), (4β)-bis(trimethylsiloxy) chlolest-5-ene*	33.179	456, 403
42	Desmosterol (TMS)	33.254	129, 343, 441, 456
43	Cholesta-3,5-dien-7-one*	33.429	458, 382, 174
44	5-Cholesten-(3β), (7α)-diol, di-trimethylsilyl	33.861	456, 546
45	Unidentified compound	33.992	73, 290, 355
–	(3β)-Trimethylsiloxy-(5α), (6α)-epoxycholestane*	34.174	95, 384, 474
46	Unidentified compound	34.249	253, 393, 498
–	(3β)-Trimethylsiloxy-(5α), (6α)-epoxycholestane*	34.393	95, 384, 474
47	Lanost-8-en-3-ol (3β) (TMS)	34.468	395, 485, 500
48	(3β)-Lanosta-7,9(11),24-trien-3-ol (TMS)	34.787	253, 496
49	Lanosterol (TMS)	35.006	393, 483, 498
50	7-Ketocholesterol (TMS)	36.395	129, 472
51	Unidentified compound	37.608	129, 472, 528

detection of the degraded compounds could be associated with the lack of sensitivity. Therefore, a second injection of the samples was carried out in SIM mode. Table 2 shows an example of the most interesting target compounds analyzed in SIM mode. The results showed the same signal decay patterns from $t = 0$ to the following aging stages illustrated in Figure 8. This behavior corroborated that the absence of the compounds at higher aging stages belonged to compound degradation and not to a lack of sensitivity of the analysis. Therefore, the main compounds of lanolin (lanosterol, lanost-8-en-3-ol (3β), (3β)-lanosta-7, 9(11), 24-trien-3-ol, cholesterol and desmosterol) cannot be considered reliable archeological biomarkers for animal shearing in archeological samples due to their lack of persistence under conditions conductive to their degradation. However, the undefined degradation compounds can be good biomarkers once their identification and source were determined. Consequently, a deeper study of these degradation compounds must be done for their identification.

According to their degradation pattern, other possible interesting persistent biomarkers could be 1-heneicosanol and 7-ketocholesterol. With respect to the unaged sample, their signal significantly decreased over aging stages, but did not completely disappear (Figure 9).

7-ketocholesterol is an easily formed autooxidation product of cholesterol, present in significant quantities in animal origin products. It is abundant in manufactured and prolonged stored food. It is also found, although generally in smaller quantities, in traditional cooked food.[58,59] On the contrary, 1-heneicosanol is presented in medicinal plant-based products.[60,61] These sources could associate the presence of these compounds to the use of flint and obsidian pieces for activities such as hunting, meat cutting, or plant gathering in addition to shearing, showing a lack of specificity, but further research would be required and may be used as secondary biomarkers to ensure shearing.

Although no specific compounds of ovine origin were identified, a profile of different compounds, both persistent and degradation products, was obtained which may be useful for the identification of lanolin in archeological samples.

Research Article
doi.org/10.1002/cmtd.202400093
Chemistry Europe
European Chemical Societies Publishing

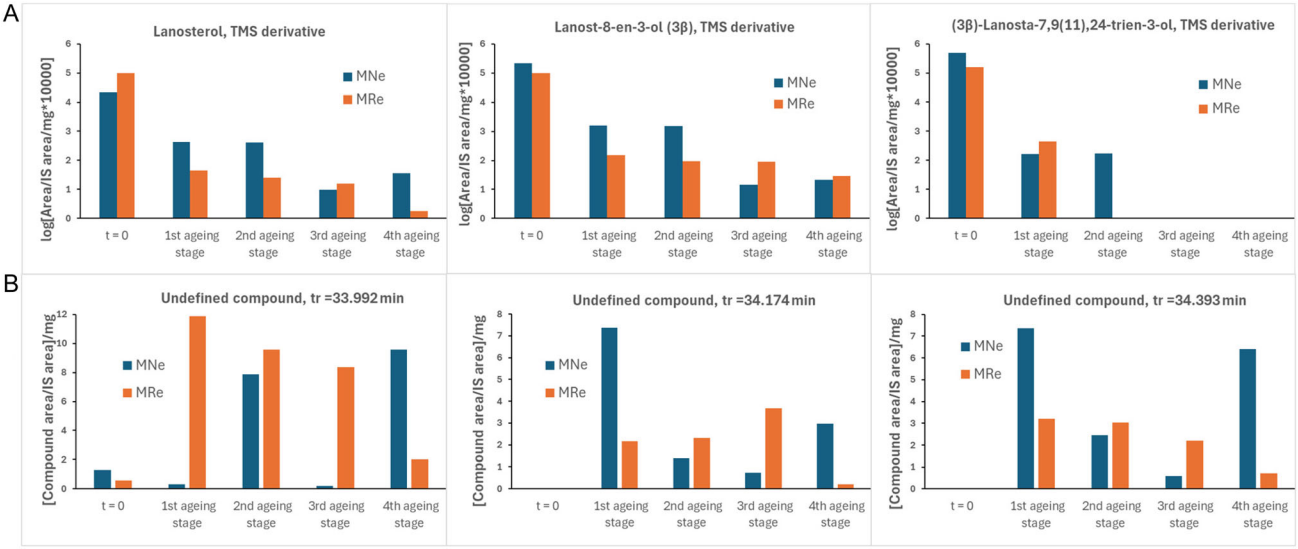

Figure 8. Characteristic compounds of natural lanolin and related compounds of interest identified in samples, as represented in Figure 7. Degradation profile over aging stages in red and black flint samples of: A) Compounds disappearing after the 1st aging stage. A multiplying factor and a logarithm transformation were applied for an improved visualization; B) Compounds appearing after 1st aging stage. Most abundant ion SIM extracted area. Internal standard and lanolin mass correction for all profiles.

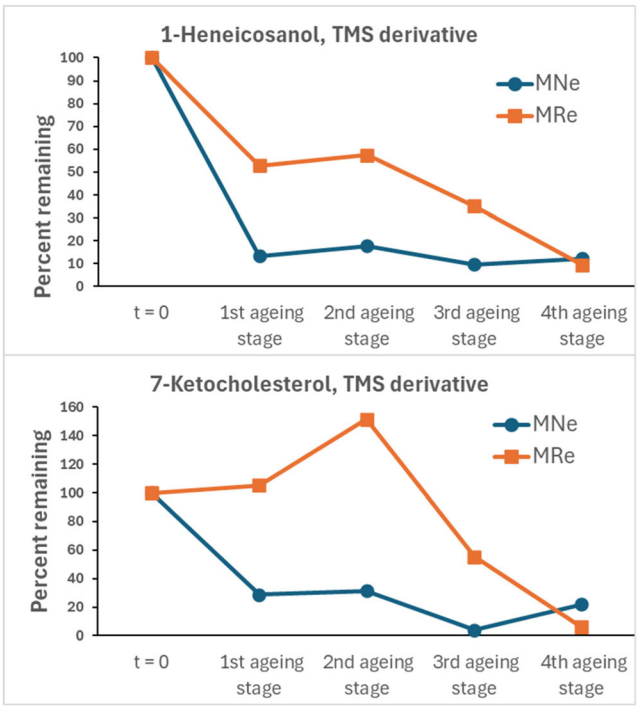

Figure 9. 1-Heneicosanol and 7-ketocholesterol degradation profiles over aging stages in red and black flint samples. The values result from the SIM extracted area of the most abundant ion, corrected with the internal standard and lanolin mass, and normalized with respect to the unaged sample ($t = 0$).

Future investigations following this archeological approach by GC-MS could start by identifying the unidentified compounds, injecting the standards of the potential analytes. The identification of these compounds could confirm or disprove the possible hypothesis about degradation patterns observed by the aforementioned techniques.

3. Conclusion

Lanolin degradation pathways have been studied by micro-FTIR in reflectance, HSI, and GC-MS.

FTIR analysis of flint and obsidian fragments before and after lanolin application showed a very different pattern, and lanolin was successfully detected. The band of the carboxyl group of fatty acid esters at 1738 cm^{-1} was the main characteristic band that hinted about degradation. Still, some spectra of lanolin-treated samples showed the shape of clean pieces spectra in both non-aged and aged samples, which are attributed to an irregular distribution of the wax on the surface, caused by its manual application.

Lanolin detection was possible by HSI in the NIR-SWIR only in black flint samples, especially in pieces presenting white areas. Therefore, it was proven that the color and gloss of the material in red flint and obsidian samples were decisive in the non-detection of lanolin by HSI in the SWIR. Yet, this scanning technique was not sensitive enough—at the value of selected concentration and on this type of surface—to detect the degradation patterns when lanolin content decrease during aging. Therefore, it can be concluded that lower detection limits can be achieved by micro-FTIR in reflectance than by HSI in the SWIR. Despite the relatively limited obtained results, HSI provided fast and useful spatial information, making it interesting as a complementary technique to the spectral information provided by FTIR.

In the future, a fast scanning of the objects by HSI could help to detect hot spots or accumulation areas of specific organic residues in archeological objects. This could serve as an exploratory phase to support possible sampling or to do a "quick-and-dirty" survey for subsequent analyses by techniques like micro-FTIR.

Finally, GC-MS analysis revealed the wide profile of lanolin, composed primarily of alcohols and fatty acids. Lanosterol, desmosterol, and cholesterol showed a significant decrease throughout ageing, showing a lack of persistence. Additional compounds

eluted at retention times close to the ones of lanosterol and detected in the aged samples suggested their formation as a consequence of the degradation of lanosterol and its derivatives. No persistent and specific potential lanolin biomarkers were identified, but a profile of many interesting compounds that could be useful to identify lanolin in archaeological samples.

This study has presented an effective analytical strategy, ready for its implementation on archaeological samples and paves the way for additional research avenues in applied analytical chemistry.

4. Experimental Section

Samples

Two types of flint samples, numbered from 1 to 5, and obsidian samples, numbered from 2 to 6, for a total of 15 samples, were named as follows.

Red flint from Sierra de Montsant (named R#, where # indicates the number of the sample) and black flint fragments from Monegros (named N#) were used. Obsidian fragments from Lipari were named O#.

Unaged lanolin-treated samples were named MR#, MN# and MO#. Lastly, aged and lanolin-treated samples were named MRe#, MNe#, and MOe#.

Blank samples (i.e., without applied lanolin) were named B# whereas the process blank for GC-MS analyses was named BP.

Acquisition of FTIR Spectra of Flint and Obsidian Samples

Three spectra were collected on one of the two sides of each fragment, selecting different zones of the surface.

Samples were analyzed in reflectance mode using a Jasco FT/IR-6300 Fourier Transform Infrared Spectrometer coupled with a Jasco IRT-7000 Irtron Infrared Microscope (Jasco Spain, Madrid), equipped with a liquid nitrogen-cooled MCT (mercury-cadmium telluride) detector. The liquid nitrogen needed was supplied by Air Liquide S.A. (Vitoria-Gasteiz, Spain). Spectra were acquired within the range 900–4000 cm^{-1} by accumulating 256 scans at a spectral resolution of 4 cm^{-1}. Spots of $100 \times 100\ \mu m^2$ were analyzed. The acquisition parameters were managed with the SpectraManager software by Jasco. Background scanning was carried out before measurement, using a polished gold surface.

Spectra were processed using Spectragryph optical spectroscopy software[62] and R 4.4.3.[63] RStudio 2024.12.1 + 563 was used as GUI for R.[64] For representing the spectra, whenever possible and sensible, the colorblind-friendly palettes Okabe-Ito[65] and viridis[66] were used. To each set of spectra, standard normal variate (SNV) preprocessing was applied and the average spectrum of all measurements taken on the black flint, red flint and obsidian fragments was calculated. FTIR reflectance spectra were then plotted in pseudo-absorbance (y-axis = log(1/R)).

Application of Lanolin on Flint and Obsidian and Acquisition and Treatment of FTIR Spectra

After the initial measurements on the bare surface, flint and obsidian fragments were manually brushed 18 times in the same direction with a 10% (w/w) lanolin solution in toluene purchased from Scharlab S.L. (Barcelona, Spain). Lanolin was obtained from Sigma-Aldrich (Steinheim, Germany). Fragments were weighed before and after the application of the lanolin solution. The mass of applied lanolin per surface area was calculated—to ensure even distribution of lanolin on the surface of the fragments—by acquiring digital images with a scale and then by using ImageJ programme.[67]

Spectra were acquired under the same conditions as mentioned above and they were pre-treated with the standard normal variate (SNV) algorithm.

Artificial Aging of Lanolin-Treated Fragments

Lanolin-treated flint and obsidian pieces were subjected to accelerated aging using a XENOCLIMA-1500 RF (CCILAB) climatic chamber (Barcelona, Spain). Four of five pieces of both types of flint and obsidian were introduced in the chamber and one of them was kept unaged. Operating conditions were: 40 °C, temperature; 70%, relative humidity; and 465.1 J m^{-2}. Radiation power was measured using a DeltaOHM HD21021 Photo-Radometer.

Samples were put in the chamber at the same time and extracted from it at different times (aging stage 1 = 8 days in the chamber; aging stage 2 = 14 days in the chamber; aging stage 3 = 21 days in the chamber; aging stage 4 = 28 days in the chamber). The samples selected for each aging stage were randomly chosen.

Hyperspectral Imaging (HSI)

Differences in sample composition were additionally evaluated by HSI. Hyperspectral analysis on unaged and aged lanolin-treated pieces was performed with a Specim NIR-SWIR camera provided by Quantum Design Europe (Barcelona, Spain). The camera operated in the 1000–2500 nm spectral range, it has 384 spatial pixels and achieves image rates of up to 400 frames per second using a CameraLink connection. The camera was mounted on a Specim LabScanner and objects under study were scanned in its $400 \times 200\ mm^2$ sample tray using halogen illumination. The scanner was controlled using the proprietary Software LUMO for Windows by Specim.

Reflectance calibration was carried out before measurements using a Spectralon tile as white reference (100% reflectance) and a dark surface reference (0% reflectance) to obtain the background spectral response.

HSI images were taken of both the lanolin-treated side and the untreated side.

Scan parameters were adjusted to observe minimal saturation on the image, resulting in an exposure time of 4.95 ms and a scanning speed of 12.5 mm s^{-1} at a working distance of 35 cm and 60 Hz frame rate.

The software used for the treatment of the hyperspectral images was Specim Spectral Imaging v. 1.3.0 build 63 for Windows.

GC-MS Analysis

Saponification, liquid–liquid extraction, and derivatisation processes were carried out on degraded lanolin pieces to be analyzed by GC-MS.

Samples were treated with 5 mL of a 2 mol L^{-1} aqueous solution of KOH in methanol (MeOH): water (10:1 v/v) purchased from Scharlab and maintained in a NÜVE FN 300 dry air sterilizer (Ankara, Turkey) at 25 °C for 24 h. MeOH was supplied from Scharlab. Water was obtained from a Milli-Q Q-POD Millipore system (Bedford, MA, US). Before extraction, 50 μL of deuterated palmitic acid ($[^2H_{31}]$-C_{16}, $C_{16\text{-}d}$, Supelco, Madrid, Spain) internal standard at a concentration of 100 mg L^{-1} in MeOH were added. Extraction was carried out by

adding 5 mL of *n*-hexane from Scharlab to the aqueous phase. The mixture was vortexed for 1 min and the supernatant phase was extracted. This process was repeated in duplicate.

The pH of the aqueous phase was adjusted below 2 using a 2 mol L^{-1} aqueous solution of HCl (37%) from Fisher Scientific (Loughborough, UK). Another extraction with 5 mL of methyl tert-butyl ether (MTBE) from Scharlab was carried out, vortexed for 1 min and the phase above was again extracted. This process was also repeated twice.

n-Hexane and MTBE phases were then combined. The combined extract was evaporated under a nitrogen current until dry and reconstituted in 1 mL of MTBE. The liquid was centrifuged for 10 min at 7000 rpm, then 100 μL were transferred to another vial and evaporated under a nitrogen current. 150 μL of pyridine and 25 μL of *N,O*-bis(trimethylsilyl)trifluoracetamide with trimethylchlorosilane (BSTFA:TMCS, 99:1 v/v) derivatising agent from Sigma-Aldrich were then added for derivatisation and samples were heated in an oven at 70 °C for 30 min. Finally, samples were analyzed by GC-MS. Analytes were separated and detected using a 8890 Gas Chromatograph System (Agilent Technologies, Madrid, Spain) coupled with a 5977B GC/MSD Mass Spectrometer and 7693 A Autosampler. The GC conditions were as follows: 1 μL was injected in splitless mode; the injector temperature was 300 °C; the column was an HP-5MS 5% Phe (30 m × 250 μm × 0.25 μm, Agilent Technologies). Helium was used as carrier gas (>99.999%, Air Liquide) at a constant column flow of 1.2 mL min^{-1}. The oven temperature was held at 90 °C for 2 min and increased to 300 °C at a rate of 7 °C min^{-1} for 20 min, and then isothermal conditions for a total run time of 42 min. MS conditions were: scan from 50 to 600 m z^{-1}; scan speed of 1.562 u s^{-1}; and frequency of 2.7 scans s^{-1}. The temperature of the transfer line was 300 °C, whereas the ion source and quadrupole temperatures were 230 and 150 °C, respectively. The electron impact ion source had an ionizing voltage of 70 eV. Another injection in SIM mode was carried out by evaporating and derivatising 400 μL of MTBE extract.

Compounds analysis and identification were managed using Agilent MassHunter software and NISTL20 compounds library, respectively.[68]

Acknowledgements

F.C. acknowledges his Maria Zambrano fellowship from UPV/EHU, funded by the Spanish Ministry of Universities and the European Union NextGenerationEU/PRTR. F.C., O.G.-L., M.R., M.M., and A.V. acknowledge support by grant TED2021-129299A-I00, funded by MICIU/AEI/10.13039/501100011033 and by the European Union NextGenerationEU/PRTR. F.C., R.J.B. and A.V. acknowledge support by grant IT1492-22 of the Basque University System. J.M.V and A.V. acknowledge support by grant PID2021-122355NB-C32 of the Spanish Ministry of Science, Innovation and University. The authors acknowledge technical and human support provided by the central service of analysis in Araba, SGIker (UPV/EHU/ERDF, EU). Open access funding provided thanks to the CRUE-CSIC agreement.

Conflict of Interest

The authors declare no conflict of interest.

Data Availability Statement

Reflectance micro-FTIR data that support the findings of this study are openly available in [Zenodo] at [10.5281/zenodo.14536650], reference number [14536651]. Other data are available from the corresponding authors upon request.

Keywords: flint · lanolin · obsidian · shearing tools · sheep shearing

[1] O. R. Dýrmundsson, *Búvísindi* **1991**, *5*, 39.
[2] M. L. Ryder, *Sheep and Man*, Duckworth & Co, London **2007**.
[3] C. G. Scanes, *Animals and Human Society* (Eds: C. G. Scanes, S. R. Toukhsati), Academic Press, Cambridge **2018**, pp. 103–131.
[4] B. S. Arbuckle, *A Companion to The Archaeology of The Ancient Near East*, John Wiley & Sons, Ltd, Chichester **2012**, pp. 201–219.
[5] E. Yurtman, O. Özer, E. Yüncü, N. D. Dağtaş, D. Koptekin, Y. G. Çakan, M. Özkan, A. Akbaba, D. Kaptan, G. Atağ, K. B. Vural, C. Y. Gündem, L. Martin, G. M. Kılınç, A. Ghalichi, S. C. Açan, R. Yaka, E. Sağlıcan, V. K. Lagerholm, M. Krzewińska, T. Günther, P. Morell Miranda, E. Pişkin, M. Şevketoğlu, C. C. Bilgin, Ç. Atakuman, Y. S. Erdal, E. Sürer, N. E. Altınışık, J. A. Lenstra, et al., *Commun. Biol.* **2021**, *4*, 1.
[6] G. Touchais, R. Laffineur, F. Rougemont, *Proc. of the 14e Rencontre égéenne internationale/14th Int. Aegean Conf., held in Paris, at the Institut National d'Histoire de l'art (INHA)*, on 11-14 December 2012, Peeters, Leuven **2014**.
[7] A. Sierra, S. Bréhard, L. Montes, P. Utrilla, M. Saña, *Archaeol. Anthropol. Sci.* **2019**, *11*, 5813.
[8] S. Sabatini, *Światowit* **2017**, *56*, 43.
[9] S. Sabatini, S. Bergerbrant, L. Ø. Brandt, A. Margaryan, M. E. Allentoft, *Archaeol. Anthropol. Sci.* **2019**, *11*, 4909.
[10] K. Grömer, *The Art of Prehistoric Textile Making: The Development of Craft Traditions and Clothing In Central Europe*, Naturhistorisches Museum Wien **2016**.
[11] E. Karimali, *The Archaeology of Mediterranean Prehistory*, John Wiley & Sons, Ltd, Chichester **2005**, pp. 180–214.
[12] M. L. Schlossman, J. P. McCarthy, *J. Am. Oil Chem. Soc.* **1978**, *55*, 447.
[13] J. S. Mills, R. White, *The Organic Chemistry of Museum Objects*, Butterworth - Heinemann, Oxford **1994**.
[14] B. Lee, E. Warshaw, *Dermatitis* **2008**, *19*, 63.
[15] B. A. Jenkins, D. V. Belsito, *Dermatitis* **2023**, *34*, 4.
[16] M. Regert, *Organic Mass Spectrometry in Art and Archaeology* (Eds: M. P. Colombini, F. Modugno), John Wiley & Sons, Ltd, Chichester **2009**, pp. 97–129.
[17] H. Pei, X. Ma, Y. Pan, T. Han, Z. Lu, R. Wu, X. Cao, J. Zheng, *J. Sep. Sci.* **2019**, *42*, 2171.
[18] R. Wolf, *Dermatology* **2009**, *192*, 198.
[19] M. P. Colombini, F. Modugno, *Organic Mass Spectrometry in Art and Archaeology* (Eds.: M. P. Colombini, F. Modugno), John Wiley & Sons, Ltd, Chichester **2009**, pp. 3–36.
[20] M. M. Hassan, H. Barker, S. Collie, *Prog. Org. Coat.* **2015**, *78*, 249.
[21] L. Cegolon, F. Larese Filon, *Life* **2024**, *14*, 916.
[22] C. Vázquez, A. Vallejo, J. M. Vergès, R. J. Barrio, *J. Archaeol. Sci. Rep.* **2021**, *40*, 103220.
[23] H. L. Whelton, S. Hammann, L. J. E. Cramp, J. Dunne, M. Roffet-Salque, R. P. Evershed, *J. Archaeol. Sci.* **2021**, *132*, 105397.
[24] D. Badillo-Sanchez, M. Serrano Ruber, A. Davies-Barrett, D. J. L. Jones, M. Hansen, S. Inskip, *Sci. Adv.* **2023**, *9*, eadh0485.
[25] R. P. Evershed, *Archaeometry* **2008**, *50*, 895.
[26] N. Dubois, J. Jacob, *Front. Ecol. Evol.* **2016**, *4*, 1.
[27] T. Brown, K. Brown, *Biomolecular Archaeology*, John Wiley & Sons, Ltd, Chichester **2011**, pp. 115–135.
[28] A. Irto, G. Micalizzi, C. Bretti, V. Chiaia, L. Mondello, P. Cardiano, *Molecules* **2022**, *27*, 3451.
[29] R. L. Feller, *Accelerated Aging: Photochemical and Thermal Aspects*, J. Paul Getty Trust, Los Angeles **1994**.
[30] C. D. Jeffra, *Archaeol. Anthropol. Sci.* **2015**, *7*, 141.
[31] M. R. Derrick, D. Stulik, J. M. Landry, *Infrared Spectroscopy in Conservation Science*, The Getty Conservation Institute, Los Angeles **1999**.
[32] B. H. Stuart, *Analytical Techniques in Materials Conservation*, John Wiley & Sons, Ltd, Chichester **2007**.
[33] I. F. Apneseth, M. Maguregui, A. Vichi, F. Caruso, *Mater. Lett* **2023**, *337*, 133963.
[34] C. Cucci, J. K. Delaney, M. Picollo, *Acc. Chem. Res.* **2016**, *49*, 2070.
[35] S. N. Cesaro, C. Lemorini, *Spectrochim. Acta A Mol. Biomol. Spectrosc.* **2012**, *86*, 299.

[36] F. Natalio, T. P. Corrales, M. Pierantoni, I. Rosenhek-Goldian, A. Cernescu, E. Raguin, R. Maria, S. R. Cohen, *Chem. Geol.* **2021**, *582*, 120427.
[37] R. F. Schmalz, *Proc. Prehist. Soc.* **1960**, *26*, 44.
[38] H. Micheelsen, *Bull. Geol. Soc. Den.* **1966**, *16*, 285.
[39] E. Kennedy, B. Sari, M. Scott, *Microsc. Microanal.* **2021**, *27*, 1850.
[40] J. N. Miller, J. C. Miller, R. D. Miller, *Statistics and Chemometrics for Analytical Chemistry*, Pearson Education Ltd., Harlow, United Kingdom **2018**.
[41] M. A. Dubé, S. Zheng, D. D. McLean, M. Kates, *J. Am. Oil Chem. Soc.* **2004**, *81*, 599.
[42] S. Agatonovic-Kustrin, G. Ramenskaya, E. Kustrin, D. W. Morton, *J. Chromatogr. B* **2021**, *1173*, 122676.
[43] S. S. Sagiri, B. Behera, K. Pal, P. Basak, *J. Appl. Polym. Sci.* **2013**, *128*, 3831.
[44] R. O. Okpuwhara, B. O. Oboirien, E. R. Sadiku, *Polym. Eng. Sci.* **2022**, *62*, 1571.
[45] M. Shanmugavel, J. Nivedha Lakshmi, S. Vasantharaj, C. Anu, L. E. Paul, R. P. Kumar, A. Gnanamani, *Biocat. Agric. Biotechnol.* **2019**, *20*, 101255.
[46] E. Lukitaningsih, M. Sa'adah, L. Purwanto, A. Rohman, *J. Am. Oil Chem. Soc.* **2012**, *89*, 1537.
[47] B. C. Smith, *Spectroscopy* **2017**, *32*, 19.
[48] K. Kaur, P. K. Yadav, G. S. Bumbrah, R. M. Sharma, *Vib. Spectrosc.* **2020**, *110*, 103146.
[49] K. Chou, B. I. Lee, *J. Mater. Sci.* **1994**, *29*, 3565.
[50] Y. Guo, Y. Zheng, S. Qiu, A. Zeng, B. Li, *J. Rare Earths* **2011**, *29*, 401.
[51] M. R. Smith, J. L. Bandfield, E. A. Cloutis, M. S. Rice, *Icarus* **2013**, *223*, 633.
[52] C. Canet, B. Hernández-Cruz, A. Jiménez-Franco, T. Pi, B. Peláez, R. E. Villanueva-Estrada, P. Alfonso, E. González-Partida, S. Salinas, *Geothermics.* **2015**, *53*, 154.
[53] K. R. Horn, *J. Archaeol. Sci. Rep.* **2018**, *21*, 10.
[54] C. Anselmi, P. Ricciardi, D. Buti, A. Romani, P. Moretti, K. Rose Beers, B. G. Brunetti, C. Miliani, A. Sgamellotti, *Stud. Conserv.* **2015**, *60*, S185.
[55] C. S. Allen, M. P. S. Krekeler, *Active and Passive Signatures*, SPIE, Bellingham **2010**, pp. 162–174.
[56] A. Castagna, H. M. Dierssen, L. I. Devriese, G. Everaert, E. Knaeps, S. Sterckx, *Remote Sens. Environ.* **2023**, *298*, 113834.
[57] *J. Am. Coll. Toxicol.* **1987**, *6*, 321.
[58] M. T. Rodriguez-Estrada, G. Garcia-Llatas, M. J. Lagarda, *Biochem. Biophys. Res. Commun.* **2014**, *446*, 792.
[59] I. Ghzaiel, K. Sassi, A. Zarrouk, S. Ghosh, I. H. K. Dias, T. Nury, M. Ksila, S. Essadek, M. T. Joutey, F. Brahmi, W. Mihoubi, S. Rup-Jacques, M. Samadi, L. Rezig, S. Meziane, T. Ghrairi, O. Masmoudi-Kouki, S. Hammami, B. Nasser, M. Hammami, Y. Wang, W. J. Griffiths, A. Vejux, G. Lizard, *Redox Exper. Med.* **2022**, *2022*, R40.
[60] V. Nautiyal, R. C. Dubey, *Saudi J. Biol. Sci.* **2021**, *28*, 2432.
[61] S. Sipriyadi, Masrukhin, R. H. Wibowo, W. Darwis, S. Yudha, I. Purnaningsih, R. Siboro, *Int. J. Microbiol.* **2022**, *2022*, 6435202.
[62] F. Menges, Spectragryph - optical spectroscopy software, v.1.2.16.1 **2022**.
[63] R Core Team, R: A language and environment for statistical computing **2025**.
[64] RStudio: Integrated Development Environment for R, PBC **2024**.
[65] Y. G. Ichihara, M. Okabe, K. Iga, Y. Tanaka, K. Musha, K. Ito, *Color Imaging XIII: Processing, Hardcopy, And Applications*, SPIE, Bellingham **2008**, pp. 206–213.
[66] S. Garnier, N. Ross, B. Rudis, A. P. Camargo, M. Sciaini, C. Scherer, viridis(Lite)- Colorblind-Friendly Color Maps for R. viridis package version 0.6.5. **2024**.
[67] C. A. Schneider, W. S. Rasband, K. W. Eliceiri, *Nat. Methods* **2012**, *9*, 671.
[68] National Institute of Standard and Technology (US), NISTL20 Compounds Library **2023**.

Manuscript received: December 20, 2024
Revised manuscript received: March 31, 2025
Version of record online: May 2, 2025